Biochimica et Biophysica Acta 1828 (2013) 405–411

Contents lists available at SciVerse ScienceDirect

Biochimica et Biophysica Acta

journal homepage: www.elsevier.com/locate/bbamem

γ-Hemolysin oligomeric structure and effect of its formation on supported lipid bilayers: An AFM Investigation

Andrea Alessandrini [a,b,*,1], Gabriella Viero [c,1], Mauro Dalla Serra [c], Gilles Prévost [d], Paolo Facci [a]

[a] Centro S3, CNR-Istituto di Nanoscienze, Via Campi 213/A, 41125 Modena, Italy
[b] Department of Physics, University of Modena and Reggio Emilia, Via Campi 213/A, 41125 Modena, Italy
[c] CNR-Institute of Biophysics & Bruno Kessler Foundation, Via alla Cascata 56/C, 38123 Trento, Italy
[d] UR EA Physiopathologie et Médecine Translationelle, Institut de Bactériologie de la faculté de médecine, 3 rue Koeberlé, 67000 Strasbourg, France

ARTICLE INFO

Article history:
Received 26 June 2012
Received in revised form 5 September 2012
Accepted 25 September 2012
Available online 1 October 2012

Keywords:
γ-Hemolysin
Atomic force microscopy
Supported lipid bilayers
Membrane curvature

ABSTRACT

γ-Hemolysins are bicomponent β-barrel pore forming toxins produced by *Staphylococcus aureus* as water-soluble monomers, which assemble into oligomeric pores on the surface of lipid bilayers. Here, after investigating the oligomeric structure of γ-hemolysins on supported lipid bilayers (SLBs) by atomic force microscopy (AFM), we studied the effect produced by this toxin on the structure of SLBs. We found that oligomeric structures with different number of monomers can assemble on the lipid bilayer being the octameric form the stablest one. Moreover, in this membrane model we found that γ-hemolysins can form clusters of oligomers inducing a curvature in the lipid bilayer, which could probably enhance the aggressiveness of these toxins at high concentrations.

1. Introduction

Membrane proteins and lipid bilayers mutually interact to accomplish many biologically relevant tasks [1–3]. It is well known that the lipid environment can modulate the functional activity of membrane proteins in several ways: i) through specific interactions between the lipids and the proteins [4]; ii) affecting the mechanical properties of the lipid bilayer, considered as a structurally organized continuum medium, and affecting conformational transitions of membrane proteins [5]; iii) mediating membrane proteins aggregation by elastic interactions [6]. The last proposed mechanism is often related to the 2D spatial organization of membrane proteins. On the other hand, the lateral organization of transmembrane proteins can lead to a re-shaping of the membrane geometry [7]. This can be accomplished by both the formation of protein scaffolds, such as in the case of BAR domains, and the shape and oligomerization of integral membrane proteins [8]. A typical case of protein-induced membrane re-shaping is represented by the chromatophores of photosyntethic purple bacteria [9].

Pore-forming-toxins (PFTs) can be considered insightful model systems to study the interaction between lipid bilayers and membrane-interacting proteins. PFTs are released in the medium as soluble monomers able to reach the surface of a lipid bilayer and to oligomerize in complex structures which span the target lipid bilayer punching holes through the target membrane [10–14]. Among the different lipid model systems that can be exploited to study the assembly and the interaction of PFTs within lipid bilayers, solid supported lipid bilayers (SLBs) provide the great advantage of being prone to be investigated by imaging surface sensitive techniques such as atomic force microscopy (AFM) [15]. With regards to PFTs and membrane/protein interaction, AFM is potentially useful to study the dynamics of the oligomer formation, the subunit composition of the oligomer and the interaction of the oligomer with the membrane. All these investigations can be performed in liquid without any prior fixation or staining procedure, providing a unique physiologic-like environment.

In this work we study by AFM the assembling and the effect on the membrane of γ-hemolysins (γHLs) oligomers exploiting SLBs in nearly physiological conditions as model membranes. γ-Hemolysin (γHL) represents one of the several β-barrel pore-forming toxins (β-PFTs) produced by *Staphylococcus aureus* [10]. At variance with the well-known homoeptameric α-hemolysin (αHL) [16], γHL is a bicomponent structure that requires the assembly of two different polypeptides belonging to the class F and class S component. Whereas the crystal structure of the oligomeric αHL is known since many years [17], only recently a crystal structure of the γHL pore in a membrane-mimicking environment has been obtained [18], providing the first case of a β-PFT for which both the soluble monomers [19–21] and pore structure have been determined by X-ray crystallography. The case of bicomponent toxins involves also the problem of the stoichiometry of the two class components in the pore structure besides the number of subunits composing the pore. The obtained crystal structure points to a pore

* Corresponding author at: Department of Physics, University of Modena and Reggio Emilia, Via Campi 213/A, 41125 Modena, Italy. Tel.: +39 059 2055297; fax: +39 059 2055651.
E-mail address: andrea.alessandrini@unimore.it (A. Alessandrini).
[1] These authors contributed equally to the work.

0005-2736/$ – see front matter © 2012 Elsevier B.V. All rights reserved.
http://dx.doi.org/10.1016/j.bbamem.2012.09.027

composed by eight subunits, instead of the seven subunits involved in the αHL structure, with a 4:4 stoichiometry of the class S and class F subunits. In previous investigations different subunit compositions with varying stoichiometry were obtained [22,23]. Interestingly, in the case of αHL the presence of both heptamers [17] and hexamers [24] in different membranes was shown. As a matter of fact, the presence of γHL octameric stable structures does not exclude the possibility of other eventually less stable subunit compositions that may occur in physiological conditions. Nonetheless, functional data clearly show that only oligomers with an equal composition of the F and S component lead to functional species [23,25], leaning towards an even stoichiometry of the pore. In general, the presence of a different number of HlgA or HlgB subunits might depend on the physico-chemical properties of the bilayer or on metastabilities of the complex but, more importantly, might unravel still unknown intermediates or non-functional oligomers along the full pore formation process.

Here we present an AFM investigation of the assembly of the two γHL components on a SLB. The investigation shows the presence of oligomers with different subunit composition. The advantage of our approach is that we do not need a purification step after oligomer formation as for X-ray crystallography and we can obtain information on the native intermediate steps toward the formation of a complete and most stable structure. Moreover, we studied how the γHL oligomer formation process affects the stability of the lipid bilayer with respect to other PFTs such as αHL.

2. Materials and methods

2.1. Preparation of lipid vesicles

Large unilamellar vesicles (LUV) with two lipid compositions, eggPC or eggPC:Chol (1:1 molar ratio), were prepared by extruding multilamellar liposome preparations through polycarbonate filters (carrying 100 nm holes). Liposomes for atomic force microscopy measurements were prepared as a 3 mg/ml lipid suspension in 10 mM Tris/HCl, 20 mM NaCl, 0.1 mM EDTA pH 7.0.

2.2. Atomic force microscopy

Supported bilayers have been prepared on mica by the vesicle fusion method at 25 °C [26]. The lipid composition most prone to permeabilization by γ-hemolysin is PC:Chol (50:50 mol%) [27]. Thus, liposomes of 100 nm diameter comprised of egg-PC:Chol (50:50 mol%) and egg-PC (as control) were used. Briefly, a liposome suspension (0.25 mg/ml) in 20 mM NaCl, 20 mM Hepes, 0.1 mM EDTA, pH 7 was applied on freshly cleaved mica for 5 minutes. The sample was then washed with the incubation buffer to remove excess of unbound liposomes. 2 μl of solutions containing either of the two classes of protein (HlgA, HlgB) were added to the supported bilayers (buffer: 20 mM NaCl, 20 mM Hepes, 0.1 mM EDTA, pH 7 or PBS; protein concentration: 200 nM). The incubation time before gentle washing to remove unbound proteins was around 2 hours at room temperature. After two hours the formation of the pores should be almost at the steady state [25,28] even though intermediates can still be seen [23]. Samples were observed with a Multimode Nanoscope IIIa (Bruker Instruments) microscope in Tapping-Mode (TM-AFM) using Oxide-sharpened Bruker NP-20 tips with a nominal spring constant of 0.24 N/m. Typically, AFM images were obtained at a scanning line speed of 1–3 Hz and the force applied was kept at its smallest possible value enabling stable imaging.

2.3. Image averaging techniques

In order to increase the signal-to-noise ratio, AFM images were processed by XMIPP software using averaging techniques [29]. Single particle images of the pores were extracted manually from the AFM micrographs. The images were then 2D aligned. Before performing an average of the images, the oligomers were analyzed by classification methods in order to identify structurally heterogeneous image sets. The classification method we used is based on Self-Organizing-Maps of the rotational spectra. This method allows identifying different classes according to the rotational symmetry. The images corresponding to each identified class were then rotationally aligned and averaged.

2.4. Aggregation effects of γHL on liposomes by fluorescence resonance energy transfer (FRET)

The ability of γHL or αHL to induce changes to the liposome structure was investigated by the probe mixing assay based on NBD–rhodamine energy transfer. To discriminate between aggregation and fusion effects, we checked the ability of each toxin to cause changes in liposome fluorescence in a probe dilution assay [30,31]. In this case a suspension of double-labeled and unlabeled liposomes were mixed together (100 μM total lipid concentration) and subjected to toxin action, both γHL (up to 100 nM) and αHL (up to 200 nM). Two different protocols were used: 1) in the probe mixing assay, two liposome preparations of eggPC/Chol in the molar ratio 1:1 and containing either NBD-DOPE or rhodamine-DOPE (2% mol) as a donor and acceptor couple for FRET, were prepared as previously described; 2) In the probe dilution assay, a liposome preparation of eggPC/Chol in the molar ratio 1:1 and containing both NBD-DOPE and rhodamine-DOPE (0.6 mol %, each) was mixed with unlabelled liposomes (eggPC/Chol, 1:1). After addition of nanomolar concentrations of toxin to the liposome suspension (0.25 mM final lipid concentration) the fluorescence emission of the donor was monitored at 535 nm for 13 min; the excitation wavelength was set to 460 nm.

3. Results and discussion

The procedure for the assembly of the Supported Lipid Bilayer allows the formation of bilayers completely covering the mica substrate. Small defects may naturally occur, enabling the measure of bilayer thickness (Fig. 1). Firstly we studied the organization features of the complex formed by the addition of the two γ-hemolysin components (HlgB and HlgA) to an already formed SLB composed by eggPC and cholesterol in the 50:50 (mol%) proportion. After incubation and washing step to remove unbound proteins, circular structures appear on the lipid bilayer (Fig. 2a) and at high resolution imaging (Fig. 2b,c), circular structures emerge more evidently. The obtained signal-to-noise ratio for each single structure clearly prevents the possibility of addressing the number of subunits constituting the oligomer. As a consequence we exploited averaging techniques to increase the signal-to-noise ratio.

Due to the circular shape of the structure of interest, the alignment should include both a 2D lateral alignment according to the center of mass and a rotational alignment according to the presence of an *n*-fold symmetry. As a first check for the presence of oligomeric structures belonging to different classes, we measured the distribution of the observed diameters. The pore diameter measured by AFM is assumed to correspond to the largest distance between the two maxima along each line intersecting the circular structure, as indicated by the dashed line in Fig. 3a. The obtained value should fall between the internal and the external diameter of the oligomeric crystal structure. The distribution of the measured diameters is reported in Fig. 3b, where a total amount of 64 single images has been considered. The distribution points out the presence of three oligomeric structures characterized by a different number of subunits, as suggested by previous investigations for the γHL structure. In fact, according to different techniques exploited to study the oligomeric structure of γHL, hexameric [32], heptameric [33] and octameric [22] subunit stoichiometries have been reported. According to these results, here we found three classes of oligomeric organizations differing in the diameter value. It is to be stressed that the presence of different classes can

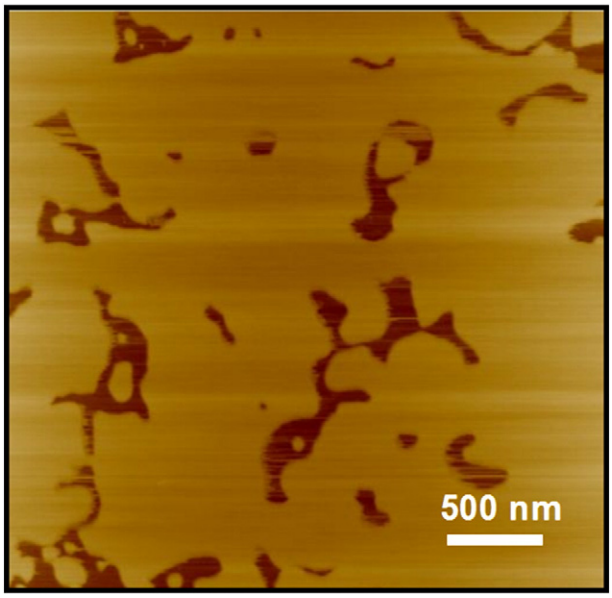

Fig. 1. AFM image of an eggPC:Cho (50:50 %mol) supported lipid bilayer obtained by the vesicle fusion technique on mica from LUV. Defects in the bilayer allow measure the thickness of the bilayer which was found to be about 6 nm.

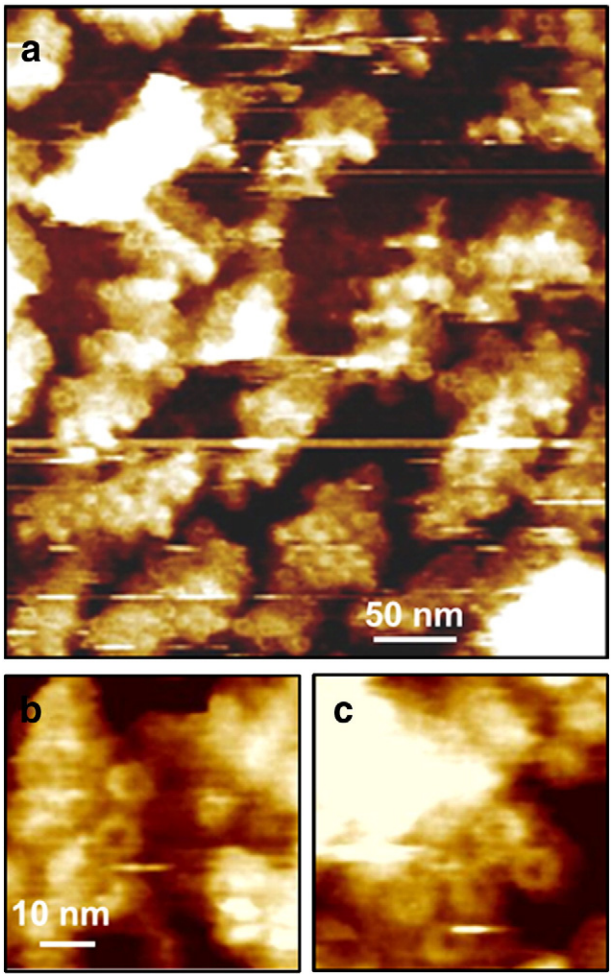

Fig. 2. a) Tapping-mode AFM (TM-AFM) image after the addition of the two components HlgA and HlgB to an eggPC:chol (50%:50%) supported bilayer; b) and c) TM-AFM images at higher resolution of the circular structures observed in a).

be considered as a sign of the physiological dynamics towards the final structure formation in which the complexes with a lower number of subunits are intermediate states on the way to the fully active pore arrangement. Moreover, at variance with other structural analysis techniques which require an initial selection of specific class of structures, here we have the possibility of observing in the same system and at the same time the presence of structures belonging to different classes. By AFM we cannot establish which one is the fully active organization and therefore, we do not know if the structures we observed represent a non-active pre-pore or the final and fully active pore configuration of the toxin.

To further characterize the three classes of oligomers emerging from Fig. 3b, we exploited the Self Organizing Map utility of the XMIPP software. The implementation of the routine is based on the rotational spectra of each single image and, in the case at issue, it shows the presence of two main classes. Next, after performing a rotational alignment of the images corresponding to each class we averaged the images. The results show that for one class both the average image and the average rotational spectra do not show any specific symmetry. The second class leads to the average image and the average rotational spectrum reported in Fig. 3c. In this case, especially from the rotational spectrum, the presence of an 8-fold symmetry is evident. Moreover, the diameter of the structure reported in Fig. 3c corresponds to the class with the largest diameter in the distribution of Fig. 3b. Fig. 3d shows an example of a single oligomer in which, even without averaging, the presence of seven subunits can be appreciated.

These results could be interpreted in the following way. The oligomers form via a sequential addition of monomers on the surface of the lipid bilayer as already established by other techniques [34]. The class with the highest number of subunits contains 8 subunits and it should represent the molecular aggregate with the most stable structure.

It has been demonstrated in vitro that the formation of functional transmembrane β-barrel displays specific energetic and structural constrains for hydrogen bonds to be formed between the neighboring β-hairpins [35,36]. Therefore, to overcome the energetic barrier for the insertion of any β-barrel into the membrane, a minimum number of monomers is required. Despite thermodynamic evaluations are not available for the HlgA/HlgB pore formation, it has been demonstrated, by using chemical cross-linking of HlgA/HlgB cysteine mutants, that concatenated dimers reproduce the WT cytolytic activity and electrophysiological pore features [23]. Indeed, the analysis of the pore conductances, after introducing exogenous negative charges within the lumen of the pore, demonstrated that four copies of each component (HlgA/HlgB couple) form functional pores, being *de facto* octamers [37]. These functional results together with our images corroborate the hypothesis that the functional pore is an octamer that probably represents the most suitable configuration for allowing a concerted and thermodynamically favorable folding configuration leading to the β-barrel insertion into the lipid bilayer

As steps towards the formation of the biggest oligomer, structures with a number of subunits lower than 8 can be found. However, the intermediate oligomers are less stable than the final one. This is likely the reason why the average image obtained from the other class identified with the Self Organizing Map classification procedure is not able to resolve the presence of individual subunits in the oligomer. The less stable structure, along with the disturbing effect of the AFM tip, could prevent a good rotational alignment of the single images for the lower subunit compositions. Even in the case of previous studies performed by transmission electron microscopy the averaging procedure performed on heptameric oligomers did not allow an increase of the signal-to-noise ratio with respect to single images [22].

The geometrical parameters of the observed octamer are consistent with the parameters extracted from the recently obtained crystal structure of the octamer. In Table 1 the geometrical parameters of the oligomeric structure obtained from AFM images in this study are reported

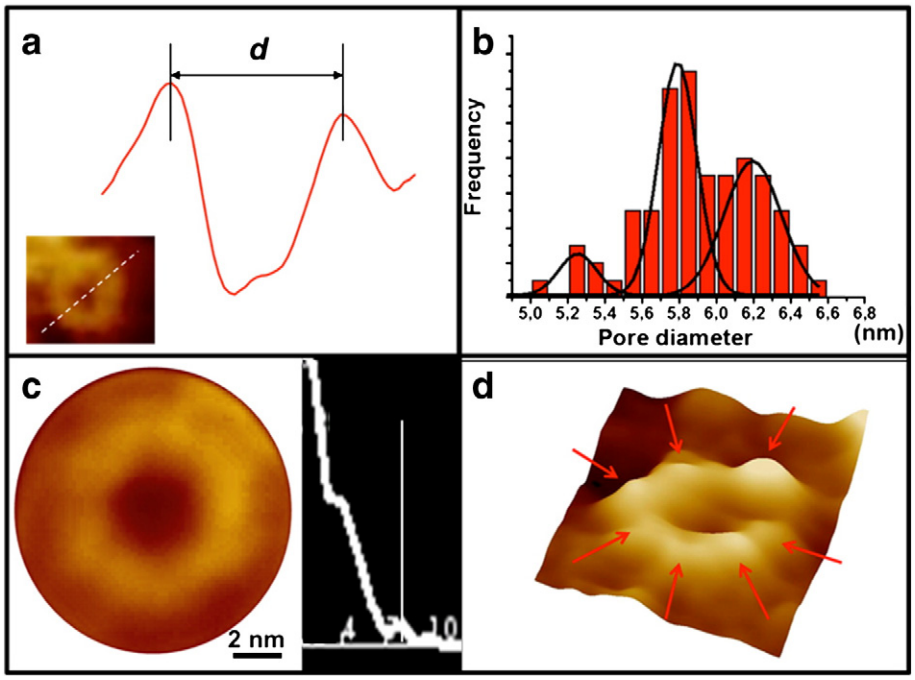

Fig. 3. a) Scheme of the measurement of the diameter *d* of each γ-hemolysin oligomer. The reported line section has been obtained along the dotted line shown in the inset; b) histogram of the measured diameters with three Gaussian fits to the emerging populations; c) average image resulting from a family identified by the Self Organizing Map routine together with the average rotational spectrum; d) example of an oligomer for which seven subunits can be identified.

and compared with the geometrical parameters of the heptameric structure of the αHL pore.

Increasing the concentration of monomers in solution, the formation of the γHL oligomers resulted in the subsequent assembling of small clusters of oligomers as shown in Fig. 4a. The hexagonal symmetry of the cluster allows establishing the distance between first neighbors in the structure. This distance could be considered as a sort of upper limit for the determination of the total diameter of the oligomeric structure. The obtained feature of 12 nm nicely agrees with the diameter obtained from the crystal structure of the octameric pore.

The appearance of small clusters of γHL oligomers has been reported in previous papers [22,38], consistently with our results. In particular, Tomita et al. reported the formation of cluster-like structures of γHL pores on the surface of erythrocyte membranes. In the same work the authors showed the breakage of the membrane around the cluster with the formation of large holes. In Fig. 4b the line section along the dashed line in Fig. 4a is reported. It is evident that the central region of the cluster is elevated with respect to the boundary region. This phenomenon could be related to a sort of curvature-induced effect of the oligomers on the lipid bilayer. In other regions of the bilayer, clusters of circular oligomers are piled up to form almost hemispherical protrusions. In Fig. 4c an example showing an almost hemispherical structure is presented. An interesting aspect is that oligomeric structures appear in regions having a height from the unperturbed bilayer of more than 10 nm (see the cross-section in Fig. 4d relative to the dotted line in Fig. 4c). The error-mode image reported in Fig. 4c (image on the right) highlights the presence of ring structures even on what could seem upstairs levels. Taking into account that oligomers can form only after the monomers have reached the bilayer surface [28,39], we must consider that all the oligomers have formed on the bilayer and then, as a consequence of the formation of a cluster, they have been raised by an induced blebbing of the lipid bilayer, as depicted in the scheme of Fig. 5, leading also to the breakage of the membrane around the cluster. The curvature measured by considering only the upper part of the sections in Fig. 4b and d is 80 μm^{-1} and 10 μm^{-1} respectively.

Table 1
Structural parameter of γHL compared to those obtained on αHL by previous AFM images.

Toxin	Diameter (nm)	Central pore (nm)	Monomer-monomer distance (nm)	Height from bilayer (nm)	Central mass distance (nm) (d in Fig. 3a)
αHL[a]	7.6 ± 0.4	2.3 ± 0.3	2.7 ± 0.3	5.0 ± 0.5	5
αHL[b]	8.9 ± 0.6	3.2 ± 0.2	2.8 ± 0.3	–	6
γHL	12[c]	3[d]	2.4 ± 0.1	4.9 ± 0.5	6.0 ± 0.1

[a] Czajkowsky, D. M., Sheng, S. T., and Shao, Z. F. (1998) J. Mol. Biol. 276, 325–330.
[b] Fang, Y., Cheley, S., Bayley, H., and Yang, J. (1997) Biochemistry 36, 9518–9522.
[c] This is calculated from the 2D crystal images and represents the upper limit of the pore diameter.
[d] This parameter relates to the averaged pore in Fig. 3c.

It is to be stressed that even in the case of αHL pores the possibility of cluster formation has been reported [40]. It has been found that the assembling of clusters of αHLs can induce the development of membrane blebs, which are released as microvesicles crowded with pores. However, the creation of vesicles has been considered in this case as a late event and not as the primary mode of membrane damage, while we cannot exclude that high doses of γHLs could induce membrane blebbing.

The proposed explanation for the observed structures could also account for the breakage of the membrane around the clusters as observed in previous works by electron microscopy [22].

Another interesting aspect of the AFM images after the incubation with the toxin and the washing procedure is the appearance of many spots in the lipid bilayer characterized by a depression of about 1 nm with respect to neighboring regions (Fig. 6). The presence of these clefts could be related to the formation of oligomers or small clusters of oligomers, which have been removed by the washing procedure. The removal of the toxins could leave a bilayer region with a lower lipid density, appearing as a depression in the AFM image. Another interpretation of the above phenomenon could be related to a lipid phase segregation induced by the oligomer formation. Both interpretations need future experiments to be discussed further.

The curvature of the lipid bilayer induced by the assembly of transmembrane proteins has been thoroughly studied both theoretically [9,41] and experimentally [42]. The induced curvature was

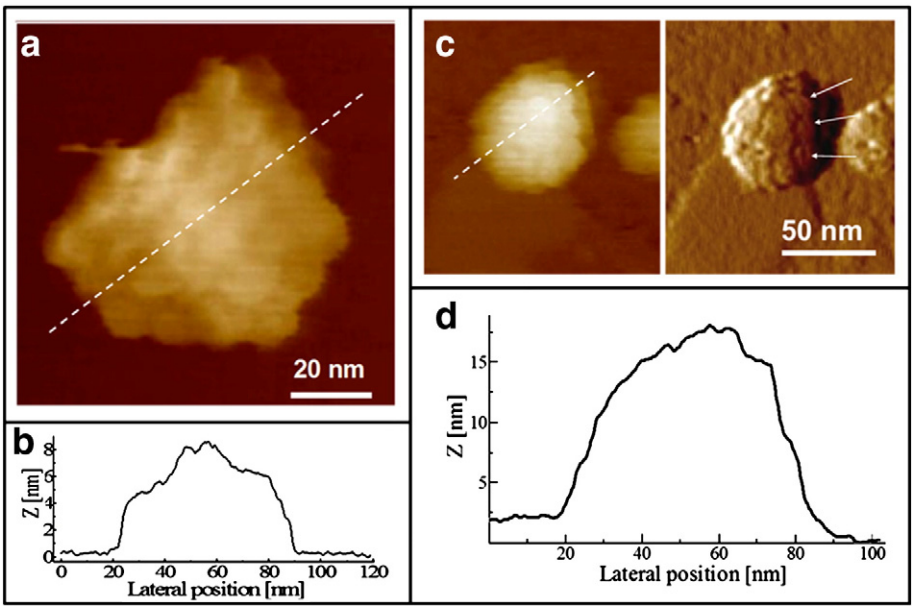

Fig. 4. a) TM-AFM image of a small cluster of γHL oligomers assembled on a supported lipid bilayer; b) cross-section of the protein cluster in a) along the dotted line; c) TM-AFM image (left) and error-mode image (right) of a small cluster of oligomers. The arrows point to the visualization of the oligomers in the cluster; d) cross-section of the protein cluster in c) along the dotted line.

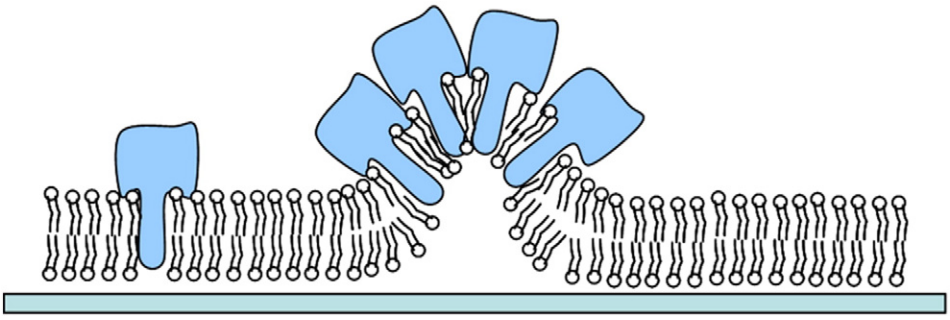

Fig. 5. Scheme of the possible mechanism for the curvature induced by the formation of oligomer clusters.

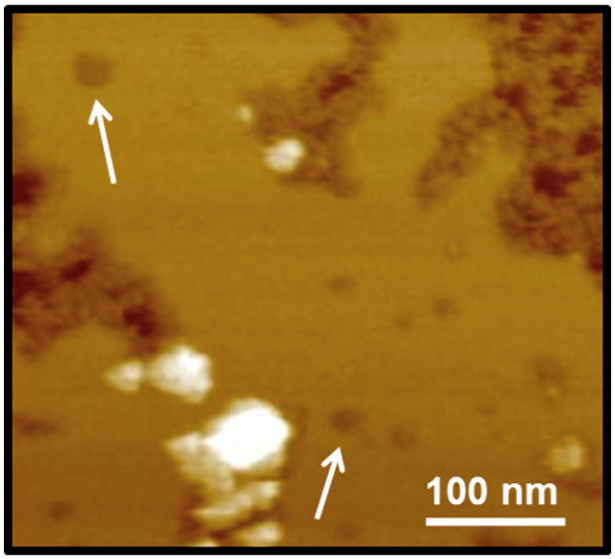

Fig. 6. TM-AFM image of a supported lipid bilayer after the incubation with the toxins and the washing step. The arrows point to the presence of small depression in the lipid bilayer.

found related to the degree of protein packing in a sort of self-reinforcement mechanism. Monte Carlo simulations suggested that asymmetry in protein size and shape represents a general driving force for the blebbing of lipid bilayers [8]. Despite experimental studies on this mechanism have been performed by AFM, this technique is usually applied on small membrane patches and the native 3D structure can be affected by alterations in the apparent membrane organization once it is transferred and forced on a flat surface [43]. In particular, the role of the membrane curvature in determining protein distribution or that of proteins in influencing the curvature may be underestimated by AFM. Olsen et al. demonstrated that the adsorption of small membrane patches containing LH2 complexes on mica can, in some cases, preserve the curvature that the patches had in solution [43]. In our case we start with a planar lipid bilayer on the solid support and we try to study whether the accumulation and clustering of oligomeric structures lead to a curvature of the lipid bilayer. The induced curvature could also explain the damage induced by γHLs on the supported lipid bilayer. In fact, the lipid bilayer does not have a reservoir of lipids and any budding configuration inevitably leads to a destruction of the membrane. This damaging effect of γHLs on the lipid bilayer is strictly related to the presence of cholesterol in the lipid mixture composing the membrane. Accordingly, in the presence of eggPC bilayer without cholesterol, both

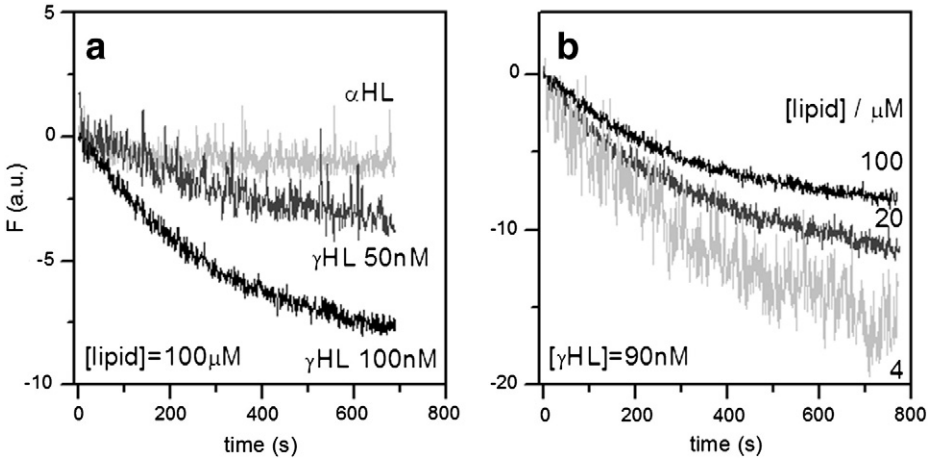

Fig. 7. Time course of liposome aggregation induced by γHL or αHL as detected in a probe mixing assay. a. Effect of γHL (50 or 100 nM) or αHL (400 nM) on the fluorescence of the donor. b. Effect of fixed amount of γHL on increasing quantity of liposomes. Other experimental conditions for both panels: buffer used was NaCl 20 mM, Tris–HCl 10 mM, EDTA 0.1 mM, pH 7.0. Observation wavelengths were set at 460 nm (excitation) and 535 nm (emission).

γ-hemolysin and α-toxin do not destabilize the supported lipid membrane (Figure S1 in the Supplementary Material). However, at variance with γHLs, αHL does not destabilize the lipid bilayer with cholesterol, being concentration conditions for the monomers equal. This difference could be related to that in the β-barrel conformation for the two pores. In fact, a truncated-cone shaped transmembrane domain could favor a curvature in the hosting lipid bilayer, whereas a cylindrical shape should not alter the curvature of a flat bilayer. The crystal structures of the two pores (γHL and αHL) show no particular difference in this region of the complex. It is however to be considered that in the crystal structure the mutual interaction between the β-barrel structure and the hydrophobic core of the lipid bilayer is not taken into account. Moreover, the different behavior of the γHL pores in the presence or absence of cholesterol suggests that also the lipid component may play a role in organizing the pores in the lipid bilayer.

Another interesting effect of the addition of Hlg to lipid bilayers is that their ability to permeabilize calcein loaded liposomes is correlated to a concentration dependent increase of PC:chol liposome dimensions, as estimated by dynamic light scattering (see Supporting Material). A different result is obtained when adding αHL to the same liposomes where no modification of liposome diameter occurs. This result demonstrates once again that Hlg consistently disorganize the homogeneity of liposomes, giving the impression that the effect could be due either to a fusion or aggregation phenomenon. Therefore, we used probe dilution and mixing assays with fluorescence resonance energy transfer (FRET) and AFM to study the effect on liposomes before and after incubation with different toxin concentrations. After addition of increasing concentration of γHL, the probe-mixing assay shows a decrease in the fluorescence intensity signal due to the toxin ability to bring the two fluorophores in close proximity. This result means that both fusion and aggregation may occur (Fig. 7a). The probe dilution assay (Fig. 7b) strongly indicates that both toxins are indeed unable to induce liposome fusion in our experimental conditions. Taken together these results provide evidences for the ability of γHL to induce aggregation. On the other hand, αHL does not induce any significant change in the detected fluorescence intensity in neither of the assays.

The size distribution of LUV was measured with AFM exploiting the vesicle fusion technique. Before and after toxin addition, liposome diameter was estimated by rupturing vesicles on freshly cleaved mica in order to form solid supported bilayers. Low concentration of lipids (0.1 mg/ml) and short incubation time (30 s) were chosen to obtain isolated bilayers ascribable to the rupturing of a single liposome. Fig. 8a shows an example of single liposomes that have ruptured on mica, forming isolated bilayer patches endowed with a quasi-circular shape. The area of the bilayers produced by single liposomes was measured and the radius of the corresponding circle of equal area was calculated. According to the preservation of the bilayer area, the corresponding liposomes in solution have a radius which is approximately half of that obtained by AFM. AFM analysis of unperturbed LUV gives a size distribution with a maximum probability for a radius

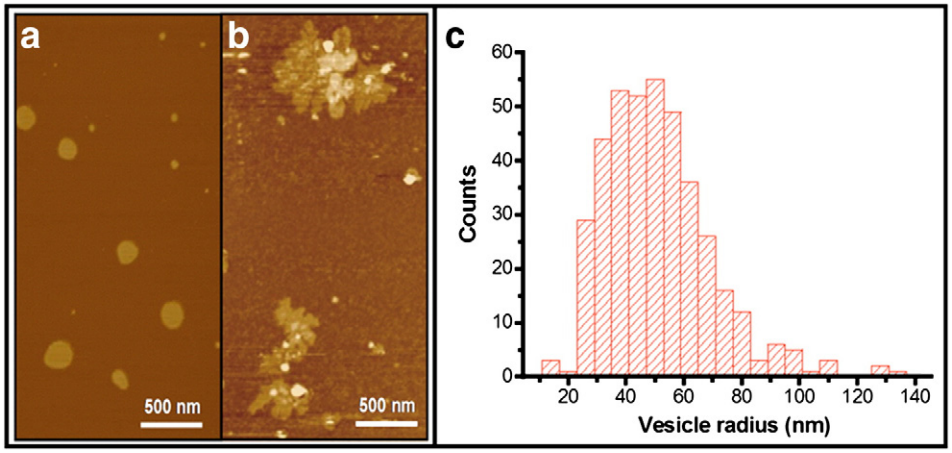

Fig. 8. a) TM-AFM image of the small patches formed by the fusion on mica of single liposomes; b) TM-AFM image resulting from the rupturing on mica of liposomes which have been exposed to Hlg monomers at a concentration allowing to form pores on the bilayer; c) vesicle radius distribution reconstructed from many images as in a).

of about 50 nm (Fig. 8c). The obtained value corresponds to what is expected for LUV prepared by extrusion through a membrane with 100 nm diameter pore size, as also measured by DLS.

Upon liposomes incubation with γHL, the rupturing of the vesicles on the mica surface results in completely different features (Fig. 8b). Surface patches with no circular symmetry are formed and the area of each structure is larger than the expected surface area for a single LUV. The obtained structures could be the result of the aggregation of liposomes in solution once γHL is added. According to the dilution and mixing probe assays results, the formation of γHL on liposomes in solution suggest a destabilization of the membrane and the formation of large aggregates.

We demonstrated that TM-AFM is able to identify the formation of oligomeric structures once γHL monomers are added to a supported lipid bilayer. High resolution imaging together with averaging techniques established that the stablest structure of the oligomer is most probably formed by eight subunits, consistently with a recently established crystal structure, but oligomers with a lower number of subunits also exist. These oligomers are probably intermediates towards the assembly of the complete pore and are less stable. Moreover, many evidences prompt that γHLs destabilize lipid bilayers in connection with their ability to form small clusters. The cluster formation probably induces a curvature in the lipid bilayer leading ultimately to vesicle budding and disruption of the membrane. The biological meaning of the destabilizing effect of the proteins on the lipid bilayer, obtained by a curvature effect resulting in the formation of budding vesicles, needs further in depth examination. In conclusion, our results suggest that pore forming toxins may be a convenient tool for studying the interplay among crowding, protein geometry, membrane domain formation and curvature.

Appendix A. Supplementary data

Supplementary data to this article can be found online at http://dx.doi.org/10.1016/j.bbamem.2012.09.027.

References

[1] R. Phillips, T. Ursell, P. Wiggins, P. Sens, Emerging roles for lipids in shaping membrane-protein function, Nature 459 (2009) 379–385.
[2] A.G. Lee, How lipids and proteins interact in a membrane: a molecular approach, Mol. Biosyst. 3 (2005) 203–212.
[3] D. Marsh, Protein modulation of lipids, and vice-versa, in membranes, Biochim. Biophys. Acta 1778 (2008) 1545–1575.
[4] A.G. Lee, The effects of lipids on channel function, J. Biol. 8 (2009) 86.
[5] J.A. Lundbaek, S.A. Collingwood, H.I. Ingolfsson, R. Kapoor, O.S. Andersen, Lipid bilayer regulation of membrane protein function: gramicidin channels as molecular force probes, J. R. Soc. Interface 7 (2010) 373–395.
[6] 'T. Gil, M.C. Sabra, J.H. Ipsen, O.G. Mouritsen, Wetting and capillary condensation as means of protein organization in membranes, Biophys. J. 73 (1997) 1728–1741.
[7] J. Zimmerberg, M.M. Kozlov, How proteins produce cellular membrane curvature, Nat. Rev. Mol. Cell Biol. 7 (2006) 9–19.
[8] R.N. Frese, J.C. Pàmies, J.D. Olsen, S. Bahatyrova, C.D. van der Weej-de Wit, T.J. Aartsma, C. Otto, C.N. Hunter, D. Frenkel, R. van Grondelle, Protein shape and crowding drive domain formation and curvature in biological membranes, Biophys. J. 94 (2008) 640–647.
[9] D.E. Chandler, J. Hsin, C.B. Harrison, J. Gumbart, K. Schulten, Intrinsic curvature properties of photosynthetic proteins in chromatophores, Biophys. J. 95 (2008) 2822–2836.
[10] G. Menestrina, M. Dalla Serra, M. Comai, M. Coraiola, G. Viero, S. Werner, D.A. Colin, H. Monteil, G. Prévost, Ion channels and bacterial infection: the case of beta-barrel pore-forming protein toxins of *Staphylococcus aureus*, FEBS Lett. 552 (2003) 54–60.
[11] S.C. Feil, G. Polekhina, M.A. Gorman, M.W. Parker, Proteins: membrane binding and pore formation. Introduction, Adv. Exp. Med. Biol. 677 (2010) 1–13.
[12] K.C. Kristan, G. Viero, M. Dalla Serra, P. Macek, G. Anderluh, Molecular mechanism of pore formation by actinoporins, Toxicon 54 (2009) 1125–1134.
[13] G. Anderluh, J.H. Lakey, Disparate proteins use similar architectures to damage membranes, Trends Biochem. Sci. 33 (2008) 482–490.
[14] I. Iacovache, F.G. van der Goot, L. Pernot, Pore formation: an ancient yet complex form of attack, Biochim. Biophys. Acta 1778 (2008) 1611–1623.
[15] A. Alessandrini, P. Facci, Unraveling lipid/protein interaction in model lipid bilayers by atomic force microscopy, J. Mol. Recognit. 24 (2011) 387–396.
[16] E. Gouaux, M. Hobaugh, L. Song, α-Hemolysin, γ-hemolysin, and leukocidin from *Staphylococcus aureus*: distant in sequence but similar in structure, Protein Sci. 6 (1997) 2631–2635.
[17] L. Song, M.R. Hobaugh, C. Shustak, S. Cheley, H. Bayley, J.E. Gouaux, Structure of staphylococcal alpha-hemolysin, a heptameric transmembrane pore, Science 274 (1996) 1859–1866.
[18] K. Yamashita, Y. Kawai, Y. Tanaka, N. Hirano, J. Kaneko, N. Tomita, M. Ohta, Y. Kamio, M. Yao, I. Tanaka, Crystal structure of the octameric pore of staphylococcal γ-hemolysin reveals the β-barrel pore formation mechanism by two components, Proc. Natl. Acad. Sci. U. S. A. 108 (2011) 17314–17319.
[19] R. Olson, H. Nariya, K. Yokota, Y. Kamio, E. Gouaux, Crystal structure of staphylococcal LukF delineates conformational changes accompanying formation of a transmembrane channel, Nat. Struct. Biol. 6 (1999) 134–140.
[20] J.D. Pedelacq, L. Maveyraud, G. Prevost, L. Baba-Moussa, A. Gonzalez, E. Courcelle, W. Shepard, H. Monteil, J.P. Samama, L. Mourey, The structure of a *Staphylococcus aureus* leucocidin component (LukFPV) reveals the fold of the water-soluble species of a family of transmembrane pore-forming toxins, Structure 7 (1999) 277–287.
[21] V. Guillet, P. Roblin, S. Werner, M. Coraiola, G. Menestrina, H. Monteil, G. Prevost, L. Mourey, Crystal structure of leucotoxin S component: new insight into the Staphylococcal beta-barrel pore-forming toxins, J. Biol. Chem. 279 (2004) 41028–41037.
[22] N. Sugawara-Tomita, T. Tomita, Y. Kamio, Stochastic assembly of two-component Staphylococcal–Hemolysin into heteroheptameric transmembrane pores with alternate subunit arrangements in ratios of 3:4 and 4:3, J. Bacteriol. 184 (2002) 4747–4756.
[23] O. Joubert, G. Viero, D. Keller, E. Martinez, D.A. Colin, H. Monteil, L. Mourey, M. Dalla Serra, G. Prévost, Engineered covalent leucotoxin heterodimers form functional pores: insights into S-F interactions, Biochem. J. 396 (2006) 381–389.
[24] D.M. Czajkowsky, S. Sheng, Z. Shao, Staphylococcal α-hemolysin can form hexamers in phospholipid bilayers, J. Mol. Biol. 276 (1998) 325–330.
[25] G. Viero, R. Cunaccia, G. Prévost, S. Werner, H. Monteil, D. Keller, O. Joubert, G. Menestrina, M. Dalla Serra, Homologous versus heterologous interactions in the bi-component staphylococcal γ-haemolysin pore, Biochem. J. 394 (2006) 217–225.
[26] A.A. Brian, H.M. McConnell, Allogeneic stimulation of cytotoxic T cells by supported planar membranes, Proc. Natl. Acad. Sci. U. S. A. 81 (1984) 6159–6163.
[27] M. Ferreras, F. Höper, M. Dalla Serra, D.A. Colin, G. Prévost, G. Menestrina, The interaction of *Staphylococcus aureus* bi-component gamma-hemolysins and leucocidins with cells and lipid membranes, Biochim. Biophys. Acta 1414 (1998) 108–126.
[28] M. Dalla Serra, M. Coraiola, G. Viero, M. Comai, C. Potrich, M. Ferreras, L. Baba-Moussa, D.A. Colin, G. Menestrina, S. Bhakdi, G. Prévost, *Staphylococcus aureus* bicomponent gamma-hemolysins, HlgA, HlgB, and HlgC, can form mixed pores containing all components, J. Chem. Inf. Model. 45 (2005) 1539–1545.
[29] C.O. Sorzano, R. Marabini, J. Velázquez-Muriel, J.R. Bilbao-Castro, S.H. Scheres, J.M. Carazo, A. Pascual-Montano, XMIPP: a new generation of an open-source image processing package for electron microscopy, J. Struct. Biol. 148 (2004) 194–204.
[30] N. Düzgünes, T.M. Allen, J. Fedor, D. Papahadjopoulos, Lipid mixing during membrane aggregation and fusion: why fusion assays disagree, Biochemistry 26 (1987) 8435–8442.
[31] D.K. Struck, D. Hoekstra, R.E. Pagano, Use of resonance energy transfer to monitor membrane fusion, Biochemistry 20 (1981) 4093–4099.
[32] M. Comai, M. Dalla Serra, M. Coraiola, S. Werner, D.A. Colin, H. Monteil, G. Prévost, G. Menestrina, Protein engineering modulates the transport properties and ion selectivity of the pores formed by staphylococcal gamma-hemolysins in lipid membranes, Mol. Microbiol. 44 (2002) 1251–1267.
[33] L. Jayasinghe, H. Bayley, The leukocidin pore: evidence for an octamer with four LukF subunits and four LukS subunits alternating around a central axis, Protein Sci. 14 (2005) 2550–2561.
[34] J. Kaneko, Y. Kamio, Bacterial two-component and hetero-heptameric pore-forming cytolytic toxins: Structures, pore-forming mechanism, and organization of the genes, Biosci. Biotechnol. Biochem. 68 (2004) 981–1003.
[35] J.H. Kleinschmidt, Folding kinetics of the outer membrane proteins OmpA and FomA into phospholipid bilayers, Chem. Phys. Lipids 141 (2006) 30–47.
[36] L.K. Tamm, H. Hong, B. Liang, Folding and assembly of beta-barrel membrane proteins, Biochim. Biophys. Acta 1666 (2004) 250–263.
[37] G. Miles, L. Movileanu, H. Bayley, Properties of *Bacillus cereus* hemolysin II: a heptameric transmembrane pore, Protein Sci. 11 (2002) 894–902.
[38] V.T. Nguyen, Y. Kamio, H. Higuchi, Single-molecule imaging of cooperative assembly of -hemolysin on erythrocyte membranes, EMBO J. 22 (2003) 4968–4979.
[39] O. Meunier, M. Ferreras, G.H.F. Supersac, L. Baba-Moussa, H. Monteil, D.A. Colin, G. Menestrina, G. Prevost, Biochim. Biophys. Acta 1326 (1997) 275–286.
[40] S. Bhakdi, J. Tranum-Jensen, Alpha-toxin of *Staphylococcus aureus*, Microbiol. Rev. 55 (1991) 733–751.
[41] B.J. Reynwar, G. Illya, V.A. Harmandaris, M.M. Müller, K. Kremer, M. Deserno, Aggregation and vesiculation of membrane proteins by curvature-mediated interactions, Nature 447 (2007) 461–464.
[42] R.P. Baumann, M. Schranz, N. Hampp, Bending of purple membranes in dependence on the pH analyzed by AFM and single molecule force spectroscopy, Phys. Chem. Chem. Phys. 12 (2010) 4329–4335.
[43] J.D. Olsen, J.D. Tucker, J.A. Timney, P. Qian, C. Vassilev, C.N. Hunter, The organization of LH2 complexes in membranes from *Rhodobacter sphaeroides*, J. Biol. Chem. 283 (2008) 30772–30779.